4-30-2022

Rotating Detonation Rocket Engine Fluidic Diode Injector Studies

Allison Brooke Lentz

Rotating Detonation Rocket Engine Fluidic Diode Injector Studies

by

Allison Brooke Lentz

An Honors Capstone

submitted in partial fulfillment of the requirements

for the Honors Diploma

to

The Honors College

of

The University of Alabama in Huntsville

30 April 2022

Honors Capstone Director: Dr. David Lineberry

Principal Research Engineer, UAH Propulsion Research Center

Allison Lentz — 04/30/2022
Student (signature) Date

David Lineberry — 04-30-2022
Director (signature) Date

D. Keith Hollingsworth — 04/30/2022
Department Chair (signature) Date

William Wilkerson Digitally signed by William Wilkerson Date: 2022.05.02 07:39:08 -05'00'
Honors College Dean (signature) Date

Honors College
Frank Franz Hall
+1 (256) 824-6450 (voice)
+1 (256) 824-7339 (fax)
honors@uah.edu

Honors Thesis Copyright Permission

This form must be signed by the student and submitted as a bound part of the thesis.

In presenting this thesis in partial fulfillment of the requirements for Honors Diploma or Certificate from The University of Alabama in Huntsville, I agree that the Library of this University shall make it freely available for inspection. I further agree that permission for extensive copying for scholarly purposes may be granted by my advisor or, in his/her absence, by the Chair of the Department, Director of the Program, or the Dean of the Honors College. It is also understood that due recognition shall be given to me and to The University of Alabama in Huntsville in any scholarly use which may be made of any material in this thesis.

Allison Lentz

Student Name (printed)

Allison Lentz

Student Signature

04/30/2022

Date

Table of Contents

Table of Figures

Dedication

For Dr. David Lineberry for his encouragement and mentorship and Dr. Gabe Xu for his mentorship as well as including me in his lab group and letting me use his stereolithography printer. For Michaela Hemming for taking me under her wing and teaching me the Cold Flow facilities and teaching me much about diodes and flow coefficients. For Garrett Cobb for always testing diodes with me and teaching me much about stereolithography printing and processing. For Jared Sauer for testing diodes with me and being a fellow Tau Bate. And For Dian “Ruthie” Hill for answering countless questions about her project that had nothing to do with mine.

Abstract

Rotating Detonation Engines are afflicted with a flashback phenomenon where the pressure of the detonation wave pushes propellants back into the propellant manifold lines. A fluidic diode integrated into the injector may mitigate such phenomenon. Two baseline fluidic diode geometries were selected from a previous work. The geometries were selected for a diodicity greater than unity. The geometries were 3D printed on a stereolithography printer as a single test article, then dilled and tapped to fit the testing facility. The testing facility was the Cold Spray facility in the Propulsion Research Center at the University of Alabama in Huntsville. The baseline diodes were tested in forward and reverse flow to capture diodicity and flow coefficients.

The fluidic diode geometry that performed higher and presented higher diodicity was selected to be integrated into a liquid rocket injector. The geometry was scaled using a method of hydraulic diameter to keep the diode passages smaller than the injector passages but prevent choking in the injector. The injectors were 3D printed in resin using a stereolithography printer. During manufacturing, two injectors failed. The remaining two injectors failed during testing. One injector burst when the system was brought up to pressure and the last failed to have liquid flow out of the article.

Chapter 1: Introduction

Liquid rocket injectors are a crucial component of a liquid rocket engine combustion chamber. Injectors introduce propellants to the combustion chamber, aid in atomizing propellants and promote mixing of the propellants for the combustion process. Large scale liquid rocket engines often have propellants distributed over hundreds of injector elements. Pressure drops in the injectors isolate the feed system from pressure oscillations in the combustion chamber.

Pressure gain combustion methods have become a topic of interest. In pressure gain combustion, the propellants are injected at low pressures into a combustion chamber where detonation processes create the high pressures necessary for producing thrust in the engine. A specific type of pressure gain combustion gaining wide interest is the Rotating Detonation Rocket Engine.

Rotating Detonation Engines (RDEs) operate by an initial detonation in a cylindrical channel that is being continuously filled with detonable propellant mixture; the detonation is free to propagate indefinitely in the channel as a wave (James Suchocki, 2012). An RDE does not contain moving parts and the engine relies on pressure gradients to continuously fill the detonation channel with a propellant mixture. The low-pressure injection in these types of engines creates challenges for injector design as well as propellant introduction into the combustion chambers.

The pressure gradients used to fill the detonation chamber and pressure differentials caused by the detonation wave create a flashback phenomenon. Flashback refers to the backflow of propellants through the injectors and into the propellant manifold lines. Flashback removes fuel from the detonation chamber and combustion within the feed system destroys the equipment (Ionio Andrus, 2017). The phenomenon causes the propagation of the detonation wave to cease, and the performance of the engine deteriorates.

The injector of the RDE uses design methods to mitigate flashback phenomenon. Lower injection areas and higher-pressure ratios contribute to optimal RDE injector design. These variables contribute to a higher injector impedance, reducing backflow potential (Thomas Teasley, 2021). Additionally, A high number of injector ports with small diameters were better for sustaining detonation. A high number of ports increased mixed and decreased backflow potential (Thomas Teasley, 2021). To improve mixing with small injector areas and high impedance, impingent injectors may be the answer. Triplet impingent injectors provide optimal mixing, higher engine performance and improved wall compatibility (Thomas Teasley, 2021).

Fluidic diodes are integrated into the injector post to increase injector impedance and reduce the back flow potential. Complex geometries encouraging flow into the combustion chamber and discouraging flow into the propellant manifold lines are modeled into the injector passages. Due to the complexity of the geometries, fluidic diode injectors are difficult to manufacture using subtractive methods. As additive manufacturing improves, fluidic diode injectors will become attainable for RDEs.

Previous Work

A Study in Diodicity of Fluidic Diode Injector Designs performed by Josie Hodges at the University of Alabama in Huntsville described Hodges's method of designing and testing fluidic diodes with the goal of reducing backflow through injectors. Four diode designs were modeled in ANSYS 3D modeling software and simulated in Spaceclaim. The simulation included a mesh sectioning of each model and calculating fluid interactions with all surfaces as well as simulating a pressurized flow through the fluidic diodes in forward and reverse direction. Once simulations concluded a greater pressure difference in the backflow direction than forward flow for all four designs, physical testing of the models was conducted (Josie Hodges, 2021).

The models were recreated in Solid Edge 3D modeling software and 3D printed using PLA plastic into a diode plate. The printed pieces were painted in a water sealant to prevent leaking and an o-ring was clamped between the printed plate and a clear plastic cover. Test conducted on the prints measured pressure up and down stream as well as mass flow across varying entrance areas. Hodges presented the calculated pressure drop and mass flow rates in forward and backwards flow for each entrance area for each diode (Josie Hodges, 2021).

Conclusions observed from Hodges's study provided the designs to begin the following study. Models were selected for their diodicity curves at the entrance areas tested in Hodges's study displayed a maximum point for diodicity was achieved. The entrance area of the diode was selected for each diode reaching a diodicty greater than unity.

Objectives

The objective of the current study was to evaluate the diodicity and flow coefficients in forwards and reverse flow of a fluidic diode incorporated into a triplet impingent injector. Injectors would be designed to a scale adaptable and compatible to a Liquid RDE. Finally, the manufacturability of the complex, small internal passaged necessary to produce the fluid diode effects are assessed.

Chapter 2: Experimental Approach

The primary steps to complete the work included selecting and fabricating baseline geometries. The selected initial geometries were printed at a large scale using a stereolithography printer. Printing on the stereolithography printer allowed the design to be printed in one piece improving sealing of the test articles over the previous work. The test articles were also processed through wet sanding and clear coat paints to allow a clear surface to investigate the diode. Next, the baseline geometries were characterized through cold flow testing. The diodicity of the baseline designs were determined by flowing water at multiple flow rates in both forward and reverse directions. Then, a geometry was selected based on the results of the baseline testing. The selected geometry is incorporated into injector passages. Injectors were fabricated on a stereolithography printer and modified through traditional subtractive machining processes where necessary to adapt to the test facility. Finally, the liquid injector was evaluated through cold flow testing with forward and reverse flow to assess the flow coefficient and diodoicity of the design to scale.

Baseline Design

Diode baseline designs were selected from Hodges' study of diodicity. The "Christmas tree" design and the "duck feet" diode were selected for their diodicity curves had reached a defined maximum and had a diodicity greater than unity at the maximum at differing entrance areas. Figure 1 displays the CAD of the Christmas tree design with a cover to make a article a single piece. Figure 2 presents the CAD of the duck feet design modified to include a cover in the single article. The remaining designs tested in Hodges' study exhibited much variation in diodicity with entrance area and these diodes had not reached their maximum diodicity in the scope of the study. An entrance area equal to half the original entrance area of the model was

selected because both the selected designs demonstrated a diodicity of greater than unity at that point.

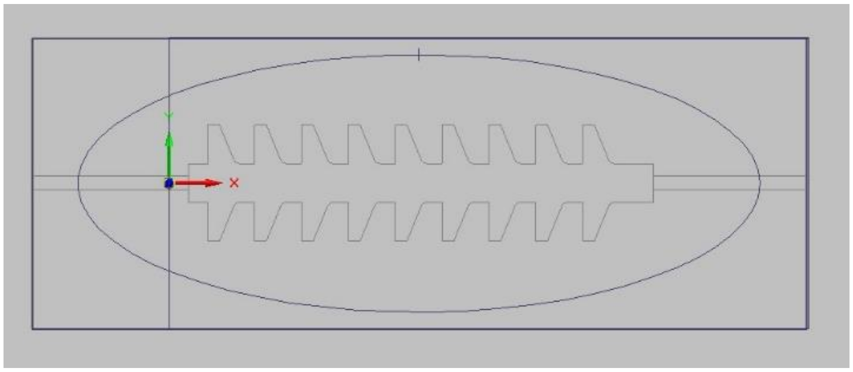

Figure 1. CAD design of "Christmas tree" diode.

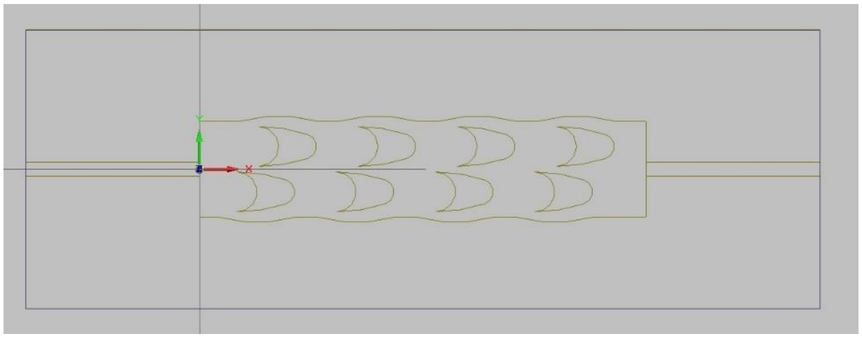

Figure 2. CAD design of "duck feet" diode.

Designs were modeled in Solid Edge 3D CAD software and the entrance areas of the selected models were reduced to half the area to capture the greatest diodicity in each design relating to Hodges' study. A plate was modeled on top of the diode baseline plate to create a single piece and reduce pressure and water losses in testing. The designs were then printed on a FormLabs 3 printer, a stereolithography printer, in resin. The diode plates were processed through polishing with wet sanding and sprayed with a clear coat prior to entering the heated curing chamber. The ends of the printed blocks were drilled and tapped for compatibility with the test facility as shown in Figure 3.

Figure 3. Resin printed baseline designs.

Experimental set up

The Cold Flow Spray Facility at the University of Alabama in Huntsville (UAH) Propulsion Research Center provided a non-reactive, high-pressure environment that simplifies set up and testing of liquid rocket engine injectors. Deionized water and nitrogen simulate propellants to characterize liquid rocket injector properties. The facility has the capability to flow water up to 3 lbm/s into either a pressurized chamber or an atmospheric spray bench. Water is pressure fed from a 60 gal. run tank to the specified testing location. High speed imaging and laser diagnostics capabilities are available with the facility. The facility contains a National Instruments data acquisition (DAQ) system for real-time monitoring and recording of pressures and temperatures throughout the system. The DAQ system collects data at 1000 Hz during a steady flow rate for 5 seconds.

The Cold Flow Spray facility in the UAH Propulsion Research Center was used for testing the diode plates. MS fittings with o-ring face seals were attached to the inlet and outlet

ports on the test article. Static pressure transducers were connected directly upstream and downstream of the test article to capture the pressure drop across the diode in forward and reverse flow. Figure 4 displays the test articles in the testing set up with pressure transducers upstream and downstream of the articles. Water mass flow rate was controlled using a 0.026 in diameter cavitating orifice. The baseline plates were tested at pressures from 0 to 600 psi in steps of 100 psi. Both designs with flow through the baseline plates are presented in Figure 5.

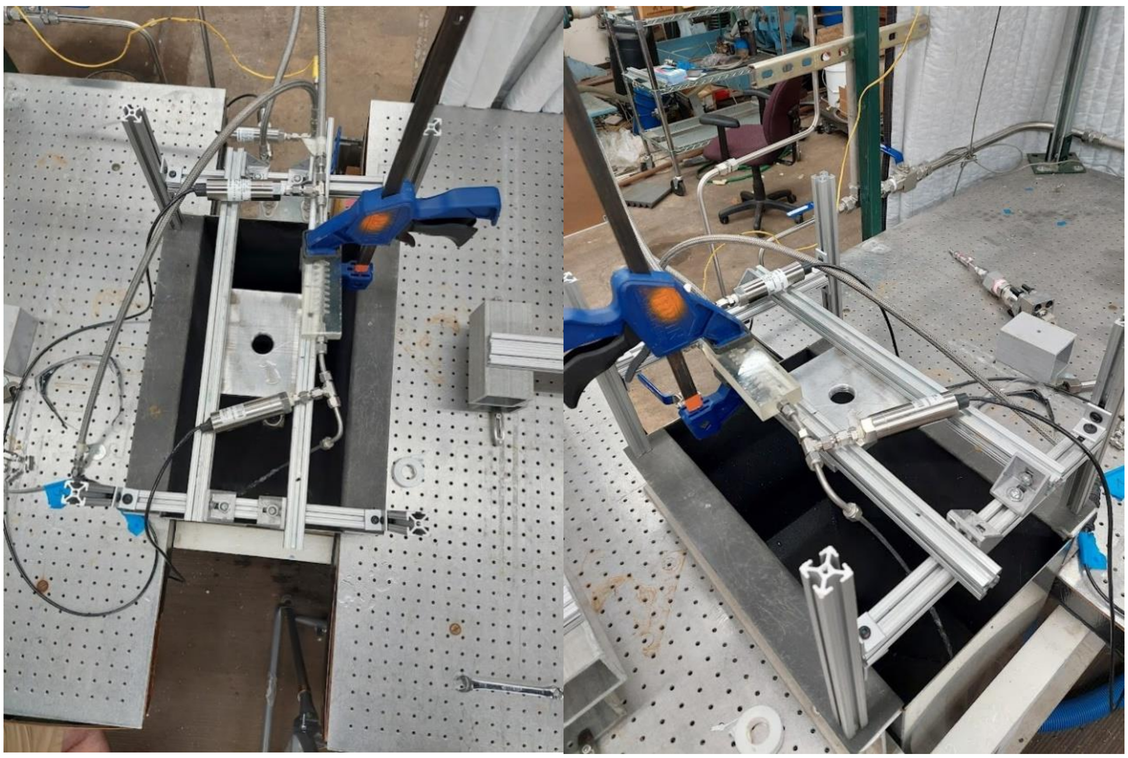

Figure 4. Cold Flow testing set up with baseline test article.

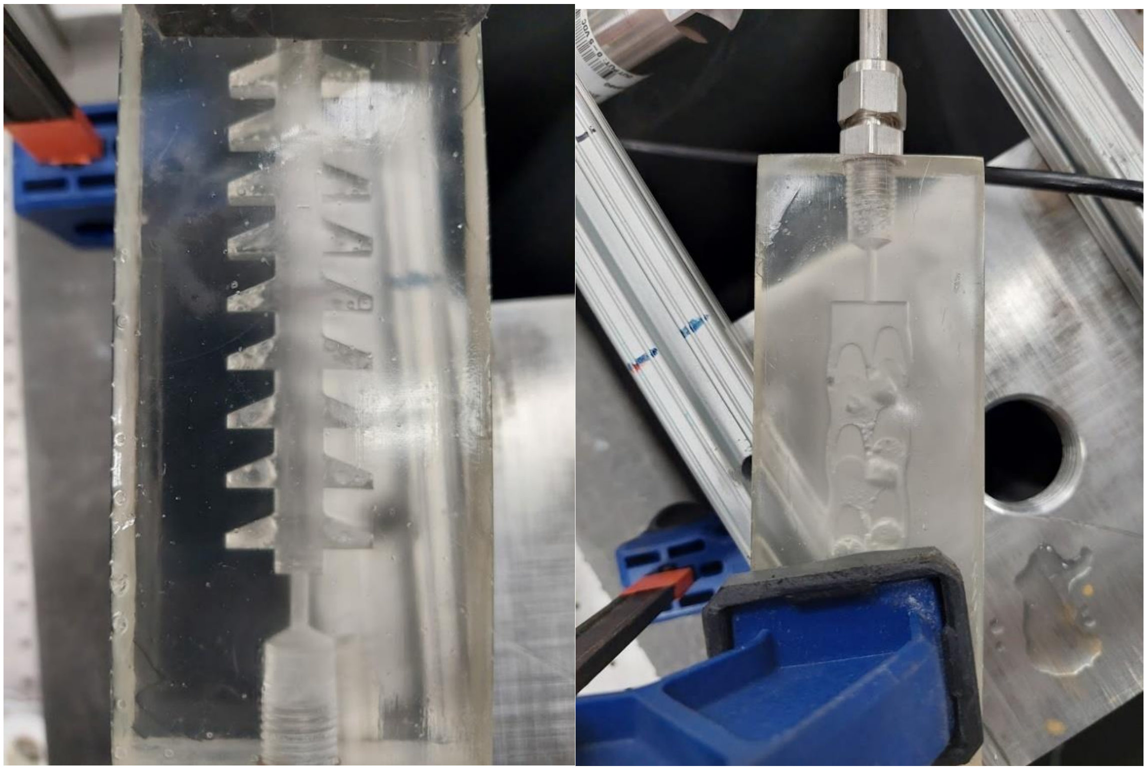

Figure 5. Flow through Christmas tree (left) and duck feet (right) baseline diodes.

Chapter 3: Results and Analysis

The LabView code associated with the Cold Flow facilities at the UAH Propulsion Research Center output the raw pressure data from pressure transducers. Pressure data values were corrected at the upstream and downstream locations by subtracting the pressure value measured at approximately 0 psi, or no flow. Upstream pressure was subtracted from the downstream pressure at the same pressure losses to determine the relative resistance the diode geometry caused in both forward and backward flow. The ratio of the pressure drop in reverse flow to pressure drop in the forward flow was calculated to determine the diodicity of both geometry at each interval the system was pressurized. Table 1 displays the diodicity of each baseline diode to the corresponding to the pressurization of the system.

Table 1. Diodicity of baseline test articles.

	Duck feet	Christmas tree
100 psi	0.9136	0.8697
200 psi	1.0104	0.9862
300 psi	1.0662	1.0164
400 psi	1.0476	0.9920
500 psi	1.0495	1.0080
600 psi	1.0470	1.0013

Observing Table 1, the duck feet baseline diode performs better than the Christmas tree diode relating to the higher diodicity values. The duck feet design retained a diodicity greater than one consistently while the Christmas tree design did not. Both baseline articles reached diodicities only slightly greater than unity meaning that the pressure difference in the reverse direction was not much greater than the forward direction. At higher pressures, and therefore higher mass flows, the baseline articles had greater diodicities. It was determined that the injector design would be tested at higher mass flow rates to achieve a greater diodicity.

Before calculating the flow coefficients, the mass flow, $\dot{m}$, through the diodes was determined with Equation 1. In Equation 1, C_d is a discharge coefficient describes an efficiency parameter to account for losses set to 0.65, typical for cavitating flow through a thin plate orifice. A is the area of the orifice; the orifice used was 0.026 in. in diameter making the area 0.000531 in^2. The density, ρ, was the density of the fluid used, water at 62.4 lbm/ft^3. Finally, pressure, P_o, was the absolute pressure of the liquid orifice in psi by adding 14.7 psi to the obtained value. The resulting mass flow results in units of lbm/min.

$$\dot{m} = C_d A\sqrt{2\rho P_o} \quad (1)$$

Table 2 exhibits the mass flow rates for both baseline articles corresponding to the pressure applied to the system. Mass flow was then converted to volumetric flow by dividing by the density of water in lbm/ft^3. By multiplying by a factor of gal/ft^3, the resulting volumetric flow was in units of gal/min. mass flow and volumetric flow were calculated at each system pressure in the forward and reverse flow directions for both models. This final volumetric flow rate was used to determine flow coefficients.

Table 2. Mass flow for both baseline designs and forward and reverse directions.

Mass flow of water in lbm/min				
	Duck Feet		Christmas Tree	
	Forward	Reverse	Forward	Reverse
100 psi	1.210	1.143	1.184	1.171
200 psi	1.620	1.607	1.612	1.611
300 psi	1.951	1.946	1.961	1.960
400 psi	2.239	2.232	2.237	2.230
500 psi	2.482	2.492	2.487	2.480
600 psi	2.713	2.715	2.730	2.714

Flow coefficient was the parameter used to compare forward and backward flow as well as diodicity to compare the different diodes to each other. This parameter has units of gallons per minute per square root of psi. Flow coefficient combines the effects of all the flow restrictions in

the fluidic diode into a single value ("Valve Sizing", 2007). The flow coefficient, C_V, equation for incompressible fluids, including water, is presented in Equation 2.

$$C_v = \frac{Q_L\sqrt{S_L}}{\sqrt{\Delta P}} \tag{2}$$

where Q_L is the volumetric flow rate of the liquid in gpm, S_L is the specific gravity of the liquid, and ΔP is the difference between the upstream and downstream pressure in psi. Table 3 displays the calculated Cv for each baseline response in forward and reverse flow.

Table 3. Flow Coefficients for both baseline geometries in forward and reverse flow.

Flow Coefficient, Cv				
	Duck Feet		Christmas Tree	
	Forward	Reverse	Forward	Reverse
100 psi	0.0966	0.0956	0.1078	0.1143
200 psi	0.1000	0.0987	0.1125	0.1132
300 psi	0.1022	0.0978	0.1147	0.1139
400 psi	0.1025	0.0999	0.1136	0.1137
500 psi	0.1026	0.1006	0.1141	0.1133
600 psi	0.1031	0.1009	0.1139	0.1132

Observing Table 3, each baseline design behaved differently. First, the duck feet diode presented lower flow coefficients overall, but consistently had a larger flow coefficient in the forward direction than the reverse direction. The duck feet design exhibited fluidic diode behavior as flow was favored in the forward direction. An additional observation of the duck feet diode is that the flow coefficient increased as pressure, and therefore mass flow, increased. This is expected behavior due to the nature of the equation. On the other hand, the Christmas tree design flow coefficients do not indicate that flow was favored in either direction, both directions had flow coefficients around the same number. Moreover, the Christmas tree design did not indicate the flow coefficient increased with mass flow. The data of the Christmas tree design in

both diodicity and flow coefficient signify no variability and the design did not indicate a successful fluidic diode.

Uncertainty Analysis

Mass flow and flow coefficient data was subject to uncertainties through the pressure transducers, the diameter of the orifice, and the discharge coefficient. The equations for mass flow and flow coefficient indicate that both parameters were subject to uncertainties from all three sources. The study in uncertainty began with the mass flow equation. Equation 3 illustrates the method to determine uncertainty in mass flow.

$$\frac{U_{\dot{m}}}{\dot{m}} = \sqrt{\left(\frac{U_{Cd}}{C_D}\right)^2 + \left(\frac{2U_d}{d}\right)^2 + \left(\frac{U_P}{2P}\right)^2} \quad (3)$$

Where C_D is the discharge coefficient, d is the diameter of the orifice, P is the pressure and U indicates an uncertainty. The uncertainty in pressure comprised of systematic and random error estimates. The manufacturer specified systematic uncertainty was 0.2% of the full-scale output of the pressure transducer, 1500 psi, making the term equal to 3 psi. In the data analysis, the systematic uncertainty can be reduced or eliminated if sensors are calibrated against the same standard or through subtracting measured values from the baseline value measured with the same sensor. In these instances, the systematic uncertainties are considered correlated and cancel in the uncertainty calculation. The random uncertainty was determined as two standard deviations of the pressure signal recorded in each five second interval. Discharge coefficient uncertainty was assumed to have a value of 0.025. The uncertainty of the diameter of the orifice was given as 0.0003 in.

Once the mass flow uncertainty was calculated, the flow coefficient uncertainty was determined. Equation 4 illustrates the method of the determining flow coefficient uncertainty.

$$\frac{U_{Cv}}{C_v} = \sqrt{\left(\frac{U_{\dot{m}}}{\dot{m}}\right)^2 + \left(\frac{-U_{\Delta P}}{2\Delta P}\right)^2} \quad (4)$$

Where this equation is dependent on the difference in upstream and downstream pressure following two standard deviation method as above. Figure 6 displays the average error in mass flow and flow coefficient in the error bars around the data points for the duck feet geometry. The uncertainty in mass flow and flow coefficient for the Christmas tree diode is found in Figure 7. The uncertainty error bars overlap for the forward and reverse directions at the same pressures for both diodes meaning it is undetermined if the data collected shows true difference between forward and reverse flow.

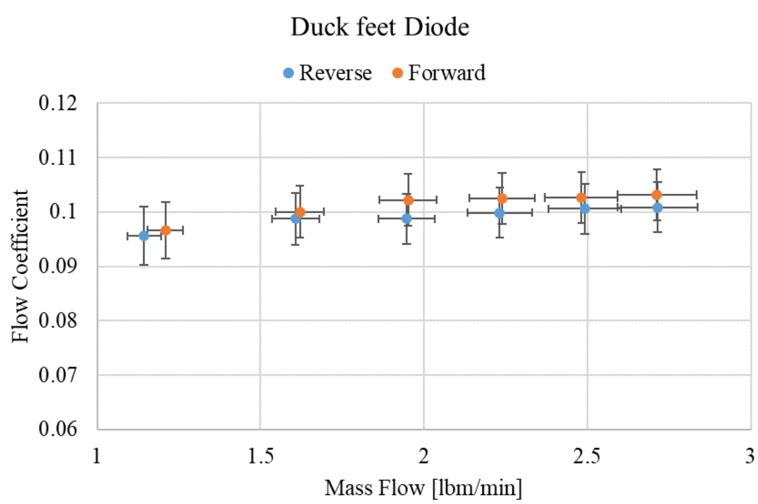

Figure 6. Reverse and Forward flow for duck feet diode with uncertainty.

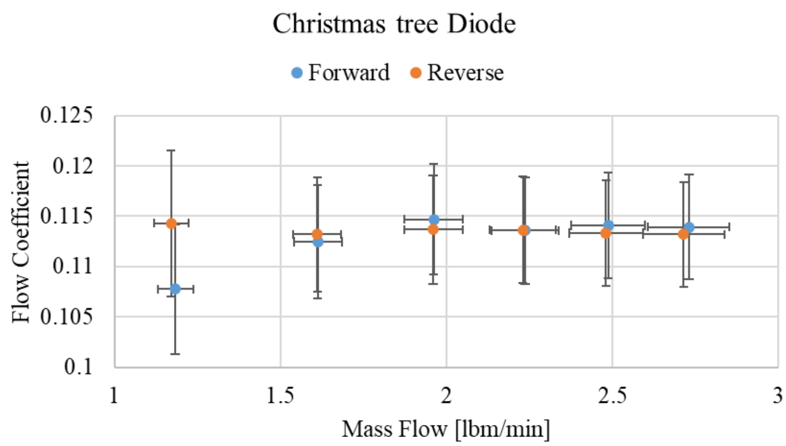

Figure 7. Reverse and Forward flow for Christmas tree geometry with uncertainty.

Injector Design and Fabrication

The design selected, the duck feet geometry, to insert into an injector design was scaled by hydraulic diameter to prevent choking the flow in the injector or the diode. The hydraulic diameter was calculated using Equation 5. The area and perimeter were calculated using simple geometries, rectangles in the case of the injector.

$$d_h = \frac{4 * Area}{Perimeter} \quad (5)$$

The minimum area in the diode was selected and scale to produce a hydraulic diameter less than the passages of the injector, but larger than the liquid orifice diameter to prevent choking. A 0.15 scale of the original diode was selected for meeting the criteria and for simplicity of scaling the diode structure. Figure 8 illustrates the cross-sectional area of the duck feet diode structure to determine hydraulic diameter. The scale selected for the hydraulic diameter was 0.736mm (0.02899 in.). The hydraulic diameter of the diode structure was less than both injector channels, 1.14 mm and 0.81 mm, but larger than the orifice, 0.026 in., to prevent choking in the injector rather than at the cavitating orifice.

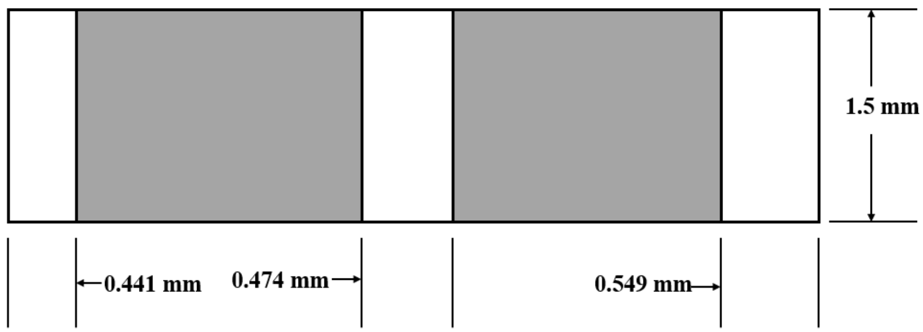

Figure 8. The final scale of the diode geometry using hydraulic diameter.

The diode structure was modeled into an existing impingent triplet injector model using Solid Edge 3D modeling software. The entire diode structure was modeled into the center post of the injector and a shortened form of the diode was inserted into the outer post due to limited space in the model. Additional models were developed included a larger diameter in the center post to improve printing and manufacturing. All three designs CAD models are illustrated in Figure 9. Three designs of the duck feet impingent triplet injector were printed using a FormLabs stereolithography printer in clear resin. One design featuring a larger center post failed during printing. Injectors were then drilled and tapped for compatibility with the Cold Flow facilities.

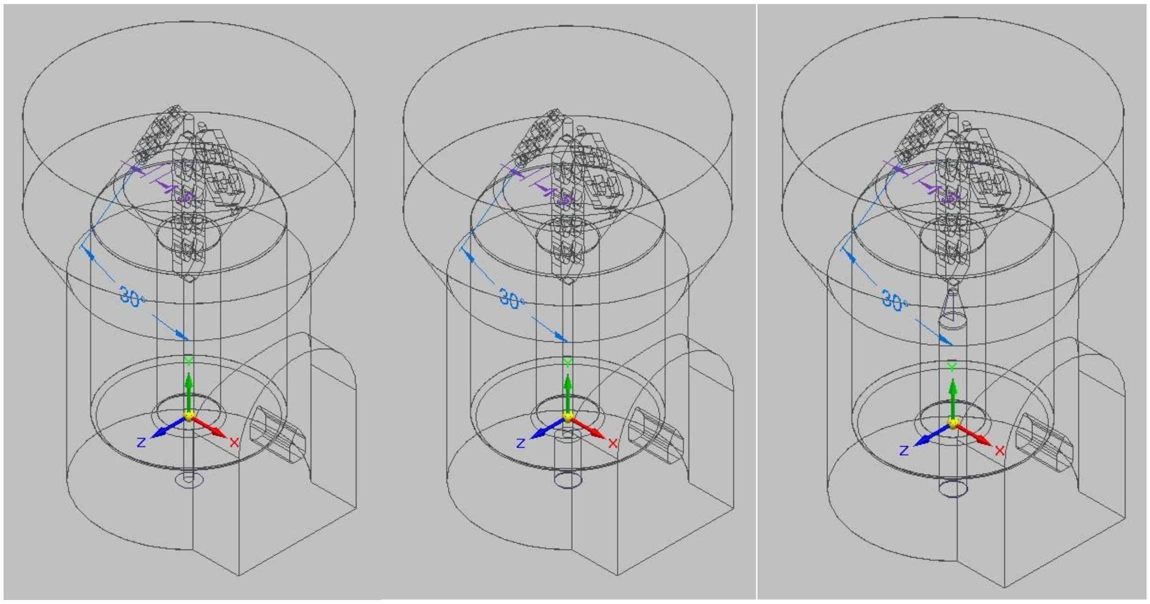

Figure 9.CAD designs of the duck foot geometry inserted into a liquid injector; Original design (left), wide entrance (center), and wide center post (right).

During drilling, the remaining injector with a large center post failed. The remaining two injectors included the original design, one cured resin and one uncured. A tapped and treaded injector is presented in Figure 10.

Figure 10. Liquid injector with integrated diode after manufacturing.

Testing

Testing the injectors involved Teflon tape applied to the fitting entering the center post due to the injector not meeting the length to drill the depth needed for the fitting and engage the o-ring. The threads on the head of the injector were Teflon tapped to ensure watertight fitting with the system for back flow testing. While bringing the system up to pressure to check for leaks, the uncured resin injector burst. It was inferred that a fitting was torqued too far into the injectors, causing a failure in the structure that was amplified with pressure addition. Figure 11 shows the test article fractured inside of the testing set up. Figure 12 displays the ruptured injector once removed from the cold flow facility. The injector fractured into two separate pieces; the injector face with the center column broke from the rest of the injector.

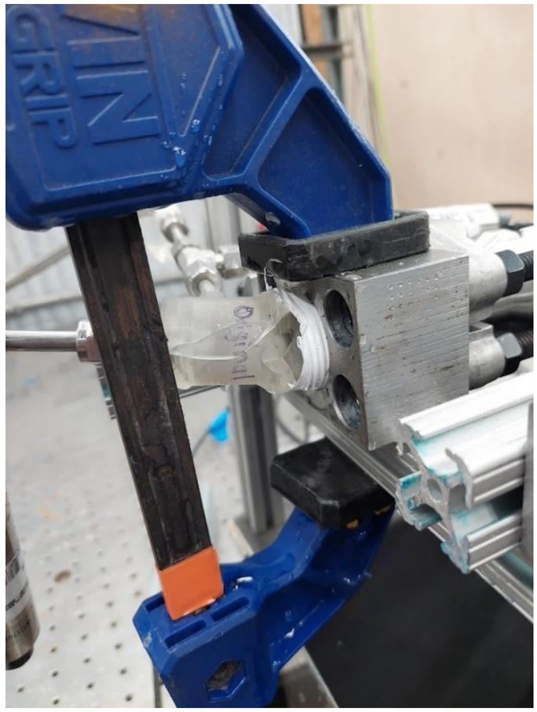

Figure 11. Failed injector within testing set up.

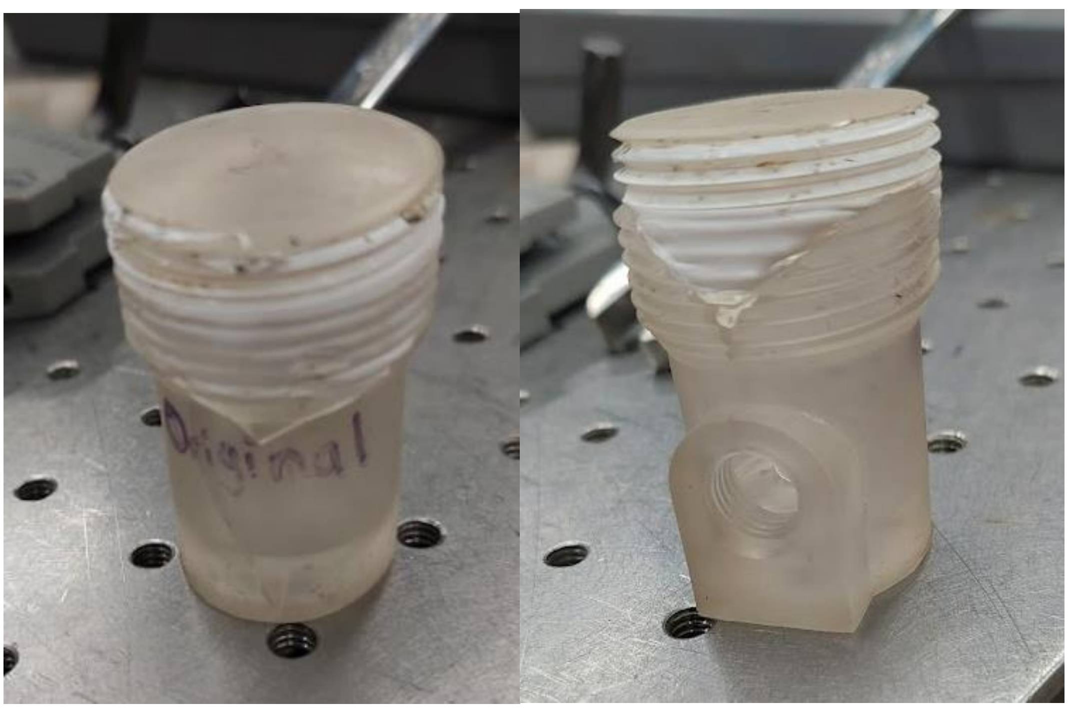

Figure 12. Failed injector shear pattern.

The cured injector was then placed into the Cold Flow facility. While checking the second injector for flow, no water flowed out of the injector. The test was shut down to prevent

pressure building in the injector and causing another burst. Water had collected inside the injector but had not escaped. It was concluded that the print failed to create a clear passage through the diode structure.

Chapter 4: Conclusion and Future Work

Two fluidic diode designs were selected as baseline geometries through previous work. The baseline diodes were 3D printed into plates using a stereolithography printer to make the articles clear and a single piece to reduce losses. Baseline plates were tested in forward and reverse flow using the University's cold flow facility. The results of the test include diodicity and flow coefficients. The duck feet geometry exhibited greater diodicity values as well as more variability between forward and reverse flow coefficient, therefore showed effects of a fluidic diode. The Christmas tree design did not perform as well and did not show any progression through changing pressures and mass flow rates. Additionally, the entrance and exit areas of the baseline diodes were selected from previous work but were very narrow. Pressure losses at the inlet and exit will dominate as they contribute to resistance in the baseline articles.

The duck feet geometry was selected to integrate into an injector. The geometry was scaled using the hydraulic diameter of the smallest area of the diode. A scale of 0.15 of the original dimensions was selected as the diameter of the diode was smaller than the passages of the injector, but larger than the cavitating orifice of the facility to prevent choking in the injector. Three injector designs were created varying the size of the center post and 3D printed in resin using a stereolithography printer. During printing, one injector failed. During manufacturing to make the injectors compatible with the facilities, another injector failed due to drilling too far into the bottom of the structure.

The remaining injectors with incorporated diodes were used for testing. The uncured resin had fittings torqued too hard into the wall and cracked the structure. While bring the testing system up to pressure, the injector fractured. The second injector, a cured resin, was integrated into the testing set up, but there was no water flow out of the injector. It was determined the print

failed within the diode structure. No data was collected from the injectors with the integrated geometry.

Future Work

Due to failures in printing may be caused by several factors. During printing, one injector fell off the build plate into the resin bath and could not be recovered. Another injector did not have clear passages to allow liquid flow through the passages. Calibrating the stereolithography printer in the facilities must be done prior to any future work as the printer has been and moved and bumped with in the facility. Print orientation of the injectors may also clear and form small passages in the injector then the orientation used in this study. The injectors may be printed at a larger scale to ensure geometry in the passages is large enough to ensure a quality print.

Additionally, the bottom surface of the injectors was not deep enough for the fittings to engage the o-ring as well as leading to another injector to fail in subtractive manufacturing. The thickness of the bottom for the flow of the center post must be lengthen prior to any future work. The baseline plates and injectors should be modeled and printed with the diameter and depth of the fittings to reduce manufacturing and failures. This would result in test articles needing only tapping, not any drilling.

During testing, the baseline plates were only testing up to 600 psi with plans to test the injectors at higher pressures and mass flow rates. Testing at higher mass flow rates would present greater differences in diodicity and flow coefficient. The data collected would make a stronger case and more data point to support the conclusions.

Diode geometries in plates proved difficult to integrate into the circular tube and cause the internal structure of the injectors to be complex. Flow must be funneled into and out of the diode structure and presented room for flow coefficient to be affected by the liquid change of

shape. Beginning with baseline designs structured for a cylindrical channel would provide data more similar to the injectors and make the geometry easily inserted into an injector.

Reference List

Ionio Q. Andrus, Paul I. King, Marc D. Polanka, Fred R. Schauer, and John L. Hoke. "Design of a Premixed Fuel–Oxidizer System to Arrest Flashback in a Rotating Detonation Engine." *Journal of Propulsion and Power* 2017 33:5, 1063-1073

James Suchocki, Sheng-Tao Yu, John Hoke, Andrew Naples, Frederick Schauer and Rachel Russo. "Rotating Detonation Engine Operation," AIAA 2012-119. *50th AIAA Aerospace Sciences Meeting including the New Horizons Forum and Aerospace Exposition*. January 2012.

Josie Hodges. "Study in Diodicity of Fluidic Diode Injector Designs." University of Alabama in Huntsville. 2021.

Thomas W. Teasley, Christopher S. Protz, Andrew P. Larkey, Benjamin B. Williams and Paul R. Gradl. "A Review Towards the Design Optimization of High Performance Additively Manufactured Rotating Detonation Rocket Engine Injectors," AIAA 2021-3655. *AIAA Propulsion and Energy 2021 Forum*. August 2021.

"Valve Sizing: Technical Bulletin." Swagelok Company. *Swagelok*. December 2007.